

Prediction of electric fields from conductors on a PCB by 3D finite-difference time-domain (FDTD) method

by W. J. Buchanan and N. K. Gupta

The finite-difference time-domain method gives accurate results for the calculation of electromagnetic wave propagation and hence can be used in a number of university final-year projects. The paper shows a novel application of the method in predicting electric fields from conductors on a PCB.

Introduction

The finite-difference time-domain (FDTD) method is extremely efficient for 3D field simulation. It may be derived directly from Maxwell's curl equations and its implementation is quite straightforward. However, the method uses a large amount of computer memory and hence its application could not be exploited generously in the past. With the advent of high-speed computers with large memory lately, the method is now showing its full potential for application in a number of areas, such as modelling of microstrip antennas, analysis of microstrip circuits, biological applications, etc. Thus the method can find wide application in university final-year engineering projects and in class-room demonstrations, some examples of which are:

- 3D wave propagation in free space
- reflections for mismatches on printed-circuit boards (PCBs)
- resonance with patch antennas
- electric and magnetic fields within and outside a substrate.

In order to encourage both staff and students to develop FDTD-related projects, this paper presents an application of the FDTD method to the prediction of electric fields from conductors on a PCB.

Time-domain simulations help to provide a better understanding of physical structures than a frequency-based analysis, which can conceal their true operations. For example, a microstrip antenna (or patch antenna) can be modelled as a transmission line or as lumped parameters. The key to understanding the antenna is to

visualise a wave reflecting back and forth within the antenna head, and electromagnetic radiation leaking out from the ends of the patch.

The finite-difference time-domain (FDTD) method

The FDTD method uses Maxwell's equations, which define the propagation of an electromagnetic wave and the relationship between the electric field, \mathbf{E} , and the magnetic field, \mathbf{H} . The equations are as follows:

$$\mu \frac{\partial \mathbf{H}}{\partial t} = -\nabla \times \mathbf{E}$$

$$\epsilon \frac{\partial \mathbf{E}}{\partial t} + \mathbf{J} = \nabla \times \mathbf{H}$$

$$\nabla \cdot \mathbf{E} = \frac{\rho}{\epsilon}$$

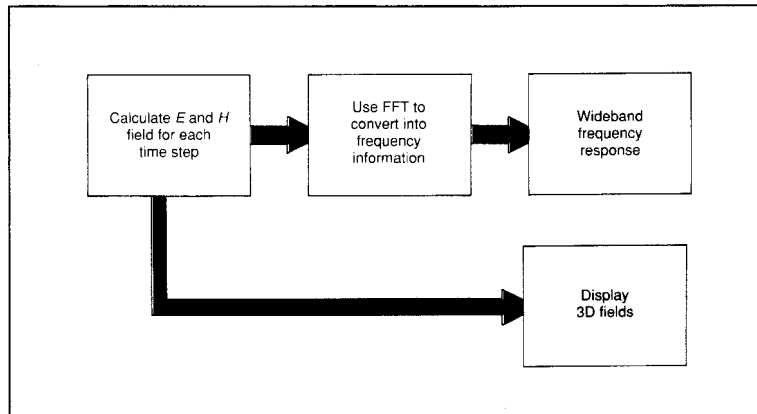
$$\nabla \cdot \mathbf{H} = 0$$

The first two equations show that a change in electric field has associated with it a magnetic field and vice versa. The third equation shows that the electric field is related to electric charge, ρ , and the last equation shows that the magnetic field relates to magnetic sources (although free magnetic poles do not exist).

The FDTD method has two main advantages over empirical analysis. Firstly, it provides a direct solution to Maxwell's equations without much complexity. Secondly, it takes into account all fields (electric and magnetic) in a three-dimensional model.

The use of parallel processing of the 3D FDTD

Fig. 1 FDTD method



method allows full time-domain solutions with frequency information extracted using fast Fourier transform techniques.

The FDTD method makes use of the increased power of today's computers to provide full time-domain solutions. Maxwell's continuous mathematical equations can be converted into a discrete form to allow them to be implemented on a digital computer. This results in the determination of frequency responses over a wide spectrum. Other methods would normally require different models and/or techniques for different frequency spectra.

For uniform, isotropic and homogeneous media with no conduction current, then Maxwell's curl equations can be simplified as:

$$\mu \frac{\partial \mathbf{H}}{\partial t} = -\nabla \times \mathbf{E}$$

$$\epsilon \frac{\partial \mathbf{E}}{\partial t} = \nabla \times \mathbf{H}$$

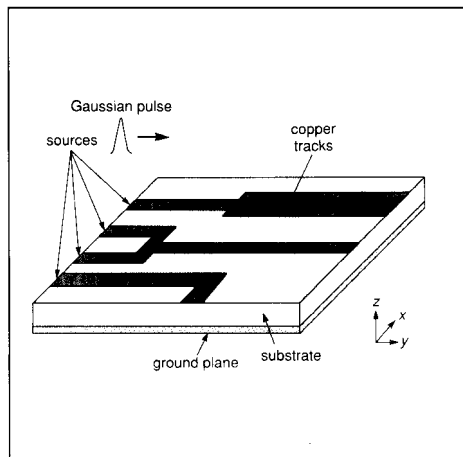


Fig. 2 PCB with copper tracks

By applying appropriate boundary conditions on sources, conductors and mesh walls an approximate solution of these equations can be found over a finite three-dimensional computational domain. As an example consider the first equation in the *i* direction:

$$\mu \frac{\Delta H_x}{\Delta t} = \frac{\Delta E_y}{\Delta z} - \frac{\Delta E_z}{\Delta y}$$

The central difference approximation is used on both the time and space first-order partial differentiations in order to obtain discrete approximations. This gives:

$$\mu \frac{H_{xi,j,k}^{n+1/2} - H_{xi,j,k}^{n-1/2}}{\Delta t} = \frac{E_{yi,j,k}^n - E_{yi,j,k-1}^n}{\Delta z} - \frac{E_{zi,j,k}^n - E_{zi,j-1,k}^n}{\Delta y}$$

Rearranging gives the following:

$$H_{xi,j,k}^{n+1/2} = H_{xi,j,k}^{n-1/2} + \frac{\Delta t}{\mu \Delta z} [E_{yi,j,k}^n - E_{yi,j,k-1}^n] - \frac{\Delta t}{\mu \Delta y} [E_{zi,j,k}^n - E_{zi,j-1,k}^n]$$

The permittivity and the permeability are set to the approximate values depending on the location of each field component. Half time steps indicate that *E* and *H* are alternately calculated in order to achieve central differences for the time derivatives. This results in six equations similar to the one given above. These define the *E* and *H* fields, in a discrete form for the *x*, *y* and *z* directions.

The 3D FDTD process is shown in Fig. 1.

Problem conception

The structure simulated in this paper is a PCB with four sources and copper tracks. Fig. 2 shows the physical structure of the PCB. It consists of a substrate layer, such as Duroid (relative permittivity of 2.2), and a ground plane below this layer. A copper layer is formed by etching the top of the substrate to give the required pattern.

This structure can be analysed using the 3D FDTD method by taking into account the following considerations.

The relative permittivities in the air above the substrate and within the substrate are ϵ_{r1} and ϵ_{r2} , respectively. At the interface between the air and the substrate, the relative permittivity is approximated as the average of the two, i.e.

$$\frac{\epsilon_{r1} + \epsilon_{r2}}{2}$$

A Gaussian pulse is applied to the source, since its frequency spectrum is also Gaussian and will provide frequency-domain information from DC to the desired cut-off frequency by adjusting the width of the pulse. This is chosen to be at least 20 points per wavelength at the highest frequency represented significantly in the pulse.

The electric field applied by the source has only a field which is perpendicular to the ground plane. Fig. 3 shows a Gaussian pulse which is delayed by 30 time steps.

Frequency information is extracted by conducting a fast Fourier transform (FFT) on the transient response. For example, to determine the reflection coefficient of the track a point is chosen at the source and the reflected wave is monitored. If the radiation pattern is required points are taken in free-space.

In the FDTD method the electrical conductors on the PCB are assumed to be perfect. The tangential electric field components that lie on the conductors are thus assumed to be zero. Fig. 4 shows that the E field components on the conductor will be zero in the x and y directions.

Six absorbing mesh boundary walls are placed around the model due to limitations in memory and speed. The ground plane and its tangential electric fields will be set to 0 and the tangential electric fields on the other five mesh walls must be specified so that a wave propagating against them does not reflect. For the structure simulated in this paper the pulses will be normally incident on the mesh walls. This leads to a simple approximation for continuous absorbing boundary conditions. The tangential fields on the

absorbing boundaries will then obey the one-dimensional wave equation in the direction normal to the mesh wall. For the normal y -direction wall the one-dimensional wave equation may be written as:

$$\left(\frac{\partial}{\partial y} - \frac{1}{v} \frac{\partial}{\partial t}\right) E_{tan} = 0$$

This equation is Mur's first approximate absorbing boundary condition and this may be made discrete to give:

$$E_0^{n+1} = E_1^{n+1} + \frac{v\Delta t - \Delta y}{v\Delta t + \Delta y} (E_1^{n+1} - E_0^n)$$

where E_0 represents the tangential electric field on the mesh wall and E_1 the field one grid point within the mesh wall. Similar equations can be derived for the other five absorbing mesh walls. This method does not take into account fringing fields which are propagating tangential to the walls. The absorbing boundary must be placed well away from any fringing fields.

The maximum time step that may be used is limited by the stability restriction of the finite-difference equations. This is shown below:

$$\Delta t < \frac{1}{c} \left[\frac{1}{\Delta x^2} + \frac{1}{\Delta y^2} + \frac{1}{\Delta z^2} \right]^{-1/2}$$

where c is the speed of light (300 000 000 m/s) and Δx , Δy and Δz are the dimensions of the unit cell.

A Fourier transform is used to extract frequency information from the transient response. The scattering parameters S_{jk} may be obtained by simple Fourier transform of the transient waveforms as

$$S_{jk}(\omega) = \frac{FF(V_j(t))}{FF(V_k(t))}$$

Results

The simulated PCB has a width of 38.9 mm, a length of 40 mm, a substrate thickness of 0.8 mm and each time-step is approximately 0.5 picoseconds. A 100 ×

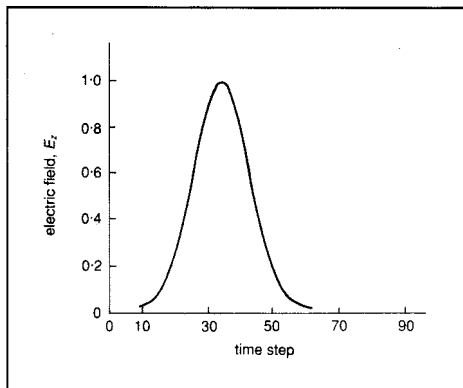


Fig. 3 Gaussian pulse

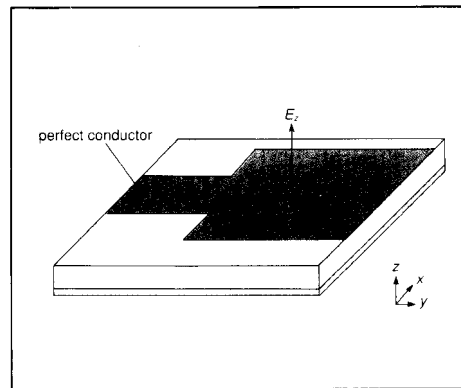
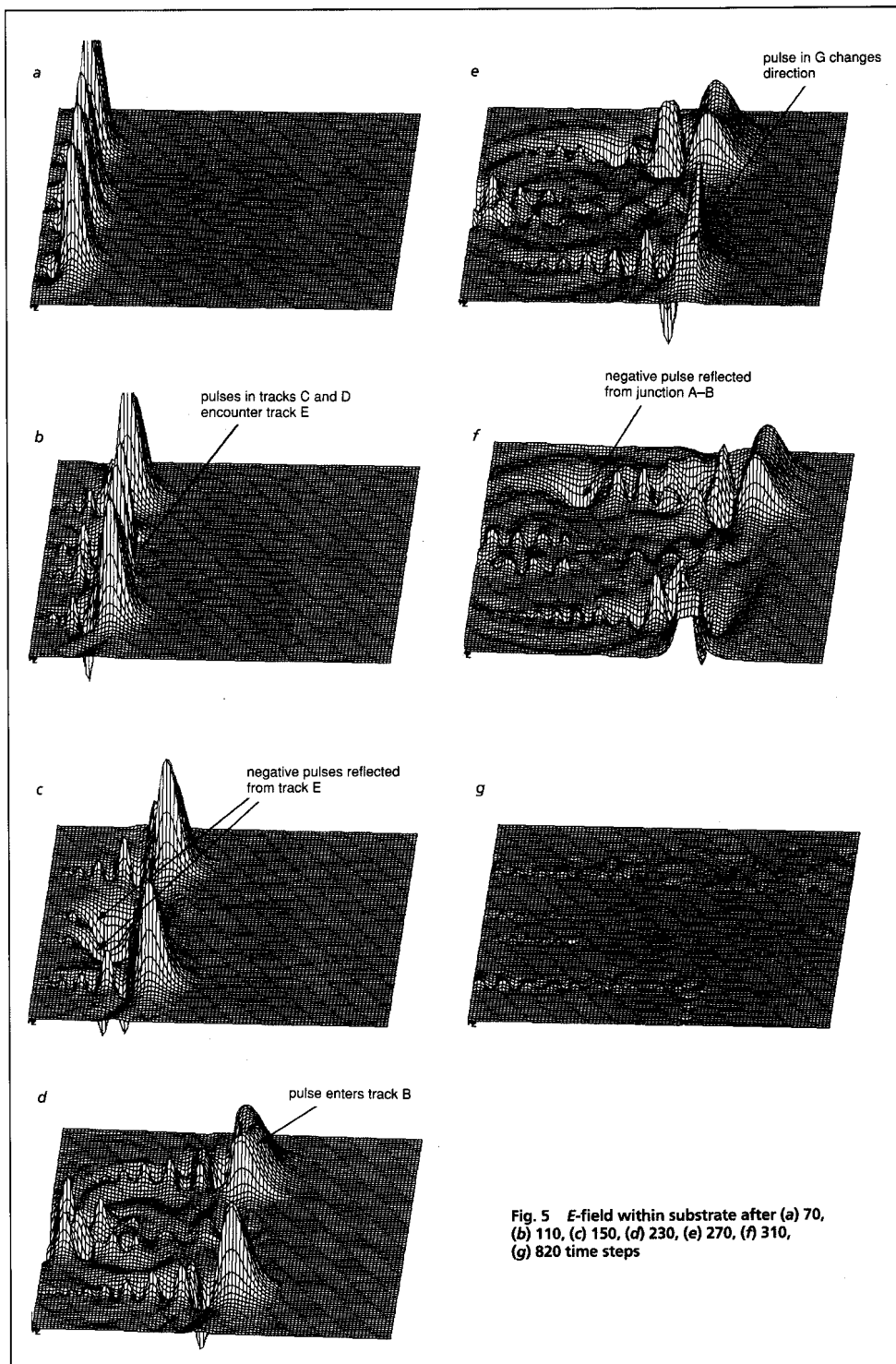


Fig. 4 Conductor treatment



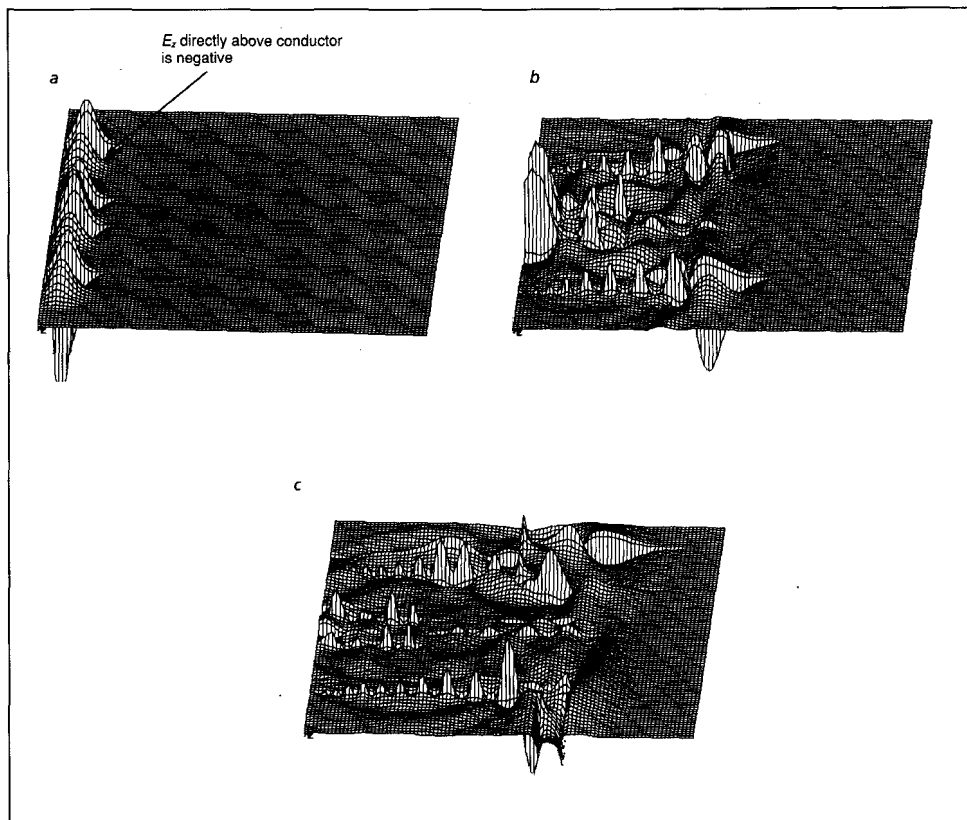


Fig. 6 E_z -field above PCB after (a) 50, (b) 210, (c) 230 time steps

100×16 grid was used for the E -field plots in the z -direction, as shown in Figs. 5 and 6. These show the electric field amplitude plots in the z -direction and are measured just above and below the copper tracks. The results were obtained using a 4-transputer array connected to a 486-based PC.

The simulation time was reduced to almost one-quarter of that for the equivalent sequential machine. A relatively small amount of time was spent with intertransputer communications. The model used assumes a match between the source and the copper tracks and an absorbing boundary around the outer walls of the problem. These values will not be totally accurate as the FDTD method does not take into account conduction or dielectric losses.

The following description relates to the track configuration of Fig. 7. Source pulses, see Fig. 5a, have entered the structure and are propagating along the tracks A, C, D and G. In Fig. 5b, the pulses within tracks C and D encounter track E. In Fig. 5c, two negative pulses are reflected from track E and propagate back through tracks C and D.

The pulse in track A enters track B and spreads outwards, as shown in Fig. 5d. A negative pulse is reflected from the junction between A and B (the

impedance of track B is less than that of A). Fig. 5e shows that the pulse travelling in track G changes direction and travels through track H. Fig. 5f shows a negative pulse travelling back along track A and the pulse travelling in track G being absorbed at the near-side wall. Fig. 5g shows that after 820 time steps all the energy has been absorbed.

Fig. 6 shows the electric field just above the PCB. The z -component of the electric field directly above the tracks will be negative as the lines of electric field point into the conductors, as illustrated in Fig. 8.

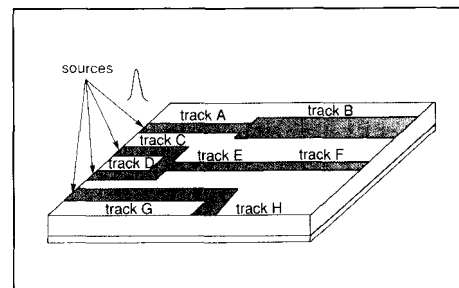


Fig. 7 Conductor treatment

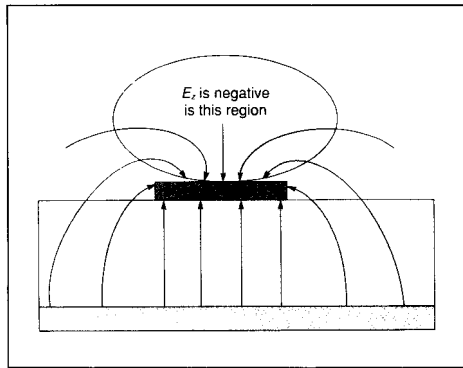


Fig. 8 Electric fields around a track

Conclusions

A novel application of the FDTD method has been shown in simulating the propagation of a Gaussian pulse applied from multiple sources within and outside a PCB. This has proved useful in showing that the electric field directly above a conductor is negative, i.e. pointing towards the conductor.

A disadvantage of the FDTD method is that it simulates structures in the time-domain. This requires a large memory storage and large run-times. However, this problem can be reduced by using modern powerful computers and for very large and complex simulations the use of parallel processing further alleviates this problem.

The results obtained clearly show the propagation and reflection of Gaussian pulses appropriate to their position in the structure and time. These can be used

to determine all required frequency characteristics from DC to the required upper frequency with no change to the model for different frequency spectra.

Acknowledgment

The authors wish to thank Professor D. Lidgate, the Head, and Professor A. E. A. Almaini, the Associate Head of the Department of Electrical, Electronic and Computer Engineering at Napier University, Edinburgh for the use of facilities.

Bibliography

- 1 SHEEN, D., ALI, S., ABOUZHARA, M., and KONG, J.: 'Application of three-dimensional finite-difference method to the analysis of planar microstrip circuits', *IEEE Trans.*, July 1990, **MTT-38**, pp.849-857
- 2 ZANG, X., FANG, J., and MEI, K.: 'Calculations of the dispersive characteristics of microstrips by the FDTD method', *IEEE Trans.*, February, 1988 **MTT-26**, pp.263-267
- 3 SHIBATA, T., HAVASHI, T., and KIMURA, T.: 'Analysis of microstrip circuits using three-dimensional full-wave electromagnetic field analysis in the time-domain', *IEEE Trans.*, June 1988, **MTT-36**, pp.1064-1070
- 4 TAFLOVE, A.: 'The finite-difference time-domain method for electromagnetic scattering and interaction problems', *IEEE Trans.*, August 1980, **EMC-22**, pp.191-202
- 5 BUCHANAN, W. J., GUPTA, N. K.: 'Parallel processing techniques in EMP propagation using 3D finite-difference time-domain (FDTD) method', *J. Advances in Engineering Software*, August 1994, **18**, (3), pp.149-159

© IEE: 1995

The authors are with the Department of Electrical, Electronic and Computer Engineering, Napier University, 219 Colinton Road, Edinburgh EH14 1DJ, UK.

IEE PROCEEDINGS: SCIENCE, MEASUREMENT AND TECHNOLOGY

Contents: May 1995

Arc modelling in SF_6 circuit breakers

J. C. V \acute{e} rit \acute{e} , T. Boucher, A. Comte, C. Delalondre, P. Robon-Jouan, E. Serres, V. Texier, M. Barrault, P. Chevrier and C. Fievet

Origin, location, magnitude and consequences of recoil in the plasma armature railgun

E. A. Witalis

Current limiting properties of an expanding helical arc

M. G. Ennis, J. K. Wood, J. Spencer, D. R. Turner, G. R. Jones and P. Coventry

Scattering matrix approach for frequency and time domain crosstalk analysis in multilayer PCBs

R. De Leo, G. Cerri and V. Mariani Primiani

Transient currents on lightning protection systems due to the indirect lightning effect

A. Karwowski and A. Zeddarn

High-frequency current transducers in a control system for quasiresonant power converters

E. Dallago and G. Sassone

Calculating the current distribution in power transformer windings using finite element analysis with circuit constraints

J.-F. Pern and S.-N. Yeh

Broadband couplers for UHF detection of partial discharge in gas-insulated substations

M. D. Judd, O. Farish and B. F. Hampton

Excitation of thick-film resonant sensor structures

N. M. White and J. E. Brignell

Fabrication of a thick film sensor employing an ultrasonic oscillator

N. M. White and G. R. Leach

New transducerless magnetic suspension system

B. V. Jayawant, R. J. Whorlow and B. E. Dawson

Covariances and invariances of the Beltrami-Maxwell postulates

A. Lakhtakis and W. S. Weighofer

Correspondence: Multidimensional Laplace transforms for solution of nonlinear equations

A. Dey and D. L. Jain